in all measurements, and errors due to (*b*) and (*c*) vary with each specimen.

Ideally, the specimen should be in the form of a focusing torus because of the beam divergence in the equatorial and axial planes. The curvatures would have to vary continuously and differently during the scan and it is impracticable to make specimens in such forms. An approximation is to make the specimen in a flexible cylindrical form with the radius of curvature increasing with decreasing 2θ (Ogilvie, 1963). This requires a very thin specimen (thus reducing the intensity) to avoid cracking and surface irregularities, and also introduces background from the substrate. A compromise uses rigid curved specimens, which match the SFC (Fig. 2.3.1.3) at the smallest 2θ angle to be scanned, and this eliminates most of the aberration (Parrish, 1968). A major disadvantage of the curvature is that it is not possible to spin the specimen.

In practice, a flat specimen is almost always used. The specimen surface departs from the focusing circle by an amount h at a distance $l/2$ from the specimen centre:

$$h = R_{\rm FC} - [R_{\rm FC}^2 - (l^2/2)]^{1/2}. \qquad (2.3.1.11)$$

This causes a broadening of the low-2θ side of the profile and shifts the centroid $\Delta 2\theta$ to lower 2θ:

$$\Delta 2\theta({\rm rad}) = -\alpha^2/(6\tan\theta). \qquad (2.3.1.12)$$

For $\alpha = 1^\circ$ and $2\theta = 20^\circ$, $\Delta 2\theta = -0.016^\circ$. The peak shift is about one-third as large as the centroid shift in the forward-reflection region. This aberration can be interpreted as a continuous series of specimen-surface displacements, which increase from 0 at the centre of the specimen to a maximum value at the ends. The effect increases with α and decreasing 2θ. The profile distortion is magnified in the small 2θ-angle region where the axial divergence also increases and causes similar effects. Typical flat-specimen profiles are shown in Fig. 2.3.1.10(*c*) and computed centroid shifts in Fig. 2.3.1.10(*d*).

The specimen-transparency aberration is caused by diffraction from below the surface of the specimen which asymmetrically broadens the profile (Langford & Wilson, 1962). The peak and centroid are shifted to smaller 2θ as shown in Fig. 2.3.1.10(*e*). For the case of a thick absorbing specimen, the centroid is shifted

$$\Delta 2\theta({\rm rad}) = \sin 2\theta/2\mu R \qquad (2.3.1.13)$$

and for a thin low-absorbing specimen

$$\Delta 2\theta({\rm rad}) = t\cos\theta/R, \qquad (2.3.1.14)$$

where μ is the effective linear absorption coefficient of the specimen used, t the thickness in cm, and R the diffractometer radius in cm. The intermediate absorption case is described by Wilson (1963). A plot of equation (2.3.1.13) for various values of μ is given in Fig. 2.3.1.10(*f*). The effect varies with $\sin 2\theta$ and is maximum at 90° and zero at 0° and 180°. For example, if $\mu = 50\,{\rm cm}^{-1}$, the centroid shift is -0.033° at 90° and falls to -0.012° at $20^\circ 2\theta$.

The observed intensity is reduced by absorption of the incident and diffracted beams in the specimen. The intensity loss is $\exp(-2\mu/x_s\,{\rm cosec}\,\theta)$, where μ is the linear absorption coefficient of the powder sample (it is almost always smaller than the solid material) and x_s is the distance below the surface, which may be equal to the thickness in the case of a thin film or low-absorbing material specimen. The thick (1 mm) specimen of LiF in Fig. 2.3.1.10(*e*) had twice the peak intensity of the thin (0.1 mm) specimen.

The aberration can be avoided by making the sample thin. However, the amount of incident-beam intensity contributing to the reflections could then vary with θ because different amounts are transmitted through the sample and this may require corrections of the experimental data. Because the effective reflecting volume of low-absorbing specimens lies below the surface, care must be taken to avoid blocking part of the diffracted beam with the antiscatter slits or the specimen holder, particularly at small 2θ.

There are additional problems related to the specimen such as preferred orientation, particle size, and other factors; these are discussed in Section 2.3.3.

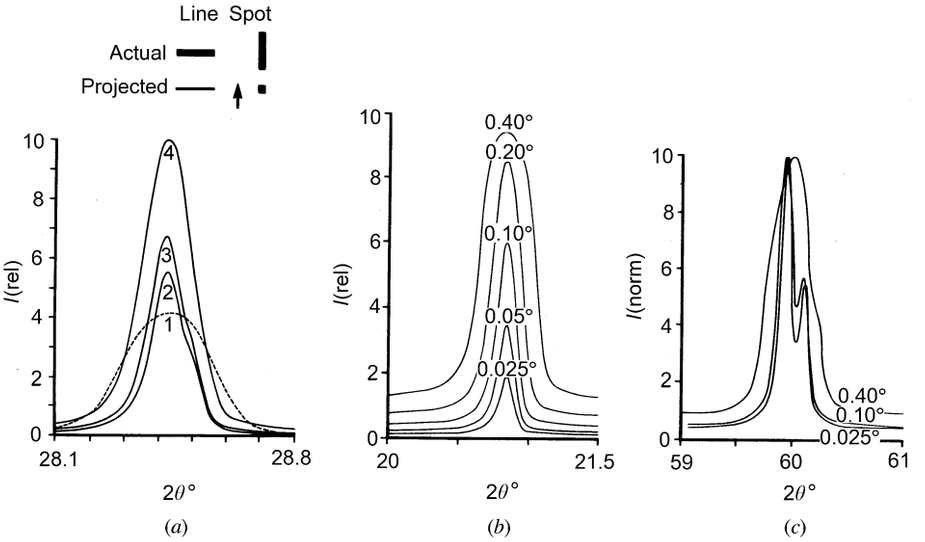

Fig. 2.3.1.9. (*a*) Effect of source size on profile shape, Cu $K\alpha$, $\alpha_{\rm ES}$ 1°, $\alpha_{\rm RS}$ 0.05°, Si(111).

No.	Projected size (mm)	FWHM (°2θ)
1	1.6 × 1.0 (spot)	0.31
2	0.32 × 10 (line)	0.11
3	0.16 × 10 (line)	0.13
4	0.32 × 12 (line)	0.17.

Effect of receiving-slit aperture $\alpha_{\rm RS}$ on profiles of quartz (*b*) (100) and (*c*) (121); peak intensities normalized, Cu $K\alpha$, $\alpha_{\rm ES}$ 1°.

references